2010 SCEC Annual Report
Systematic mapping of the Moho beneath southern California

PIs: Meghan S. Miller and James Dolan
Participating graduate student: Panxu Zhang

1 Overview

The goal of this project is to clearly define the three-dimensional geometry and depth of the Moho and lithosphere-asthenosphere boundary throughout southern California by using P receiver functions in order to systematically look for discontinuities that may be related to discrete faulting at depth. This region has a complicated tectonic history (e.g., Atwater, 1970) and therefore the three-dimension map could provide us with significant information on the geometry of the crust and lithosphere, as well as the tectonic evolution of this region. Work during the past year has focused mainly on the following two tasks: (1) systematic mapping of the Moho beneath southern California; and (2) detailed study of the Moho and the lithosphere –asthenosphere boundary (LAB) beneath the San Jacinto fault zone.

2 Data and analysis

We applied the P receiver function technique (Langston, 1977; Vinnik, 1977) to teleseismic events from 2000 to 2010 recorded by the Southern California Seismic network (Figure 1). Based on the requirements of the P receiver function method, teleseismic events with magnitude greater than 6.0 and distances between 35 to 90 degrees were selected. In the case of P receiver functions, the longitudinal component is deconvolved from the in-plane SV component to image P to S conversion at depth. This technique will provide the necessary frequency and depth resolution for both a Moho map and identification of crustal structures near major strike-slip faults. Then depth conversion was applied into the P receiver functions based on the Tectonic North America (TNA) velocity model of Grand and Helmberger (1984).

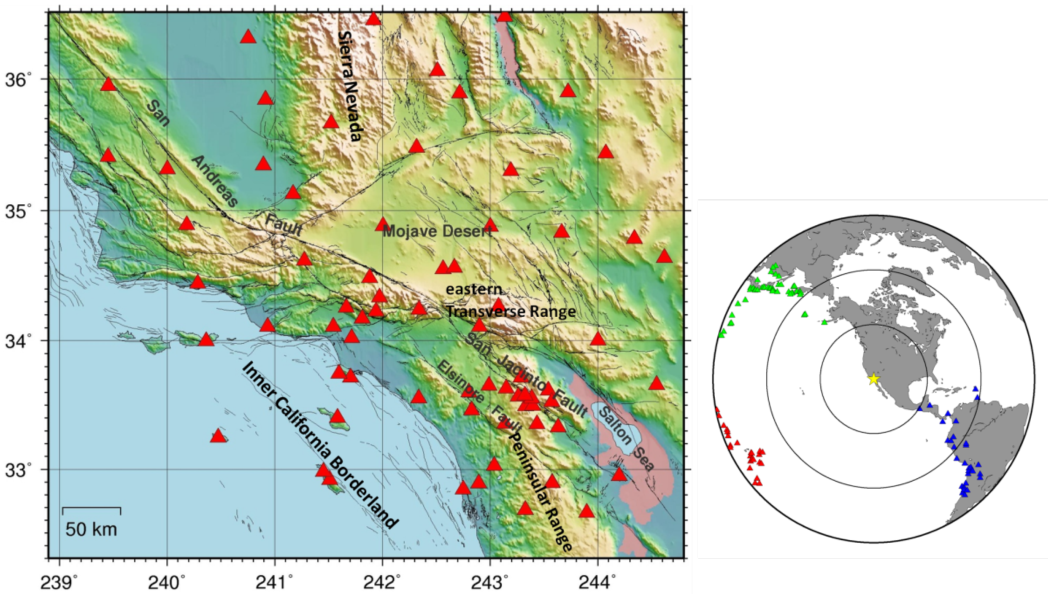

Figure 1. Ninety-seven broadband stations of the Southern California Seismic Network (SCSN) used in the study. Teleseismic events from 2000 to the present with magnitude greater than 6.0 and great circle distance between 35 to 90 degrees.

3 Variation in the Moho depth of southern California

An interpolated Moho depth map was obtained based on depth conversion results (Figure 2). The map shows clear, yet complex regional variations, with a general southeastward shallowing from ~45 km to 20 km, with an average Moho depth of ~31km. A very shallow Moho of around 20 km is observed beneath the Salton Sea and the Inner California Borderland. A relatively deep Moho of 35~40 km is observed below the Techachapi Mountains, Peninsular Ranges, and the eastern Transverse Ranges. These crustal depth variations agree with previous studies by other groups (Zhu, 2000; Yan and Clayton, 2006).

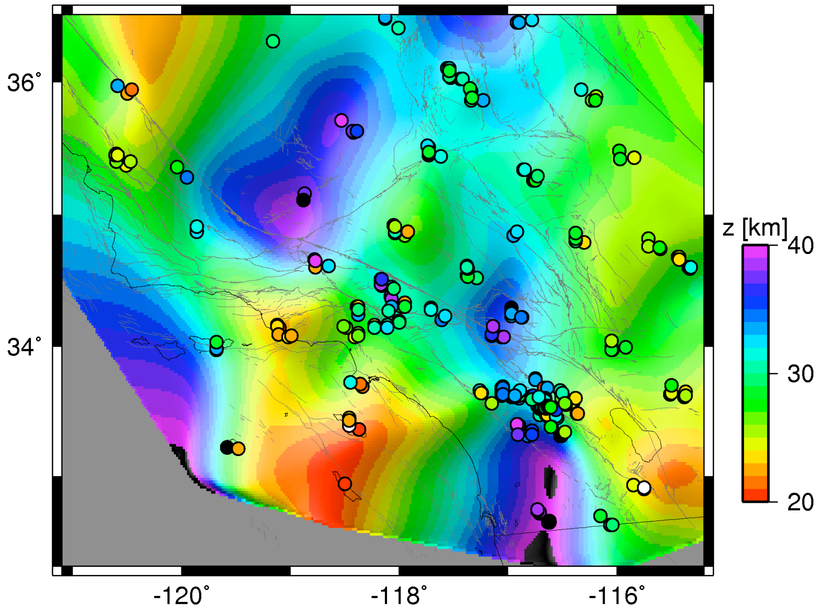

Figure 2. : Interpolated Moho depth map. Each circle represents depth data from each receiver function gather and the P-to-S conversion point at 30 km deep. Black points represent a very deep Moho with depth higher than maximal value (40km) in color bar.

4 Detailed study on the San Jacinto Fault Zone

During the past year, we have focused primarily on the San Jacinto fault zone due to the high density of seismic stations in the area and the fact that the San Jacinto fault is one of the most seismically active branches of the San Andreas fault system (Figure 3). It is not a continuous fault, but rather a fault zone, and its segments exhibit different geometries and physical properties. For example the northern, central and southern segments of the San Jacinto fault exhibit different seismicity patterns and seismogenic zone depths (Wdowinski, 2009). In particular, there is a 20 km ANZA gap that is relatively aseismic within the seismically active central segment of the San Jacinto fault.

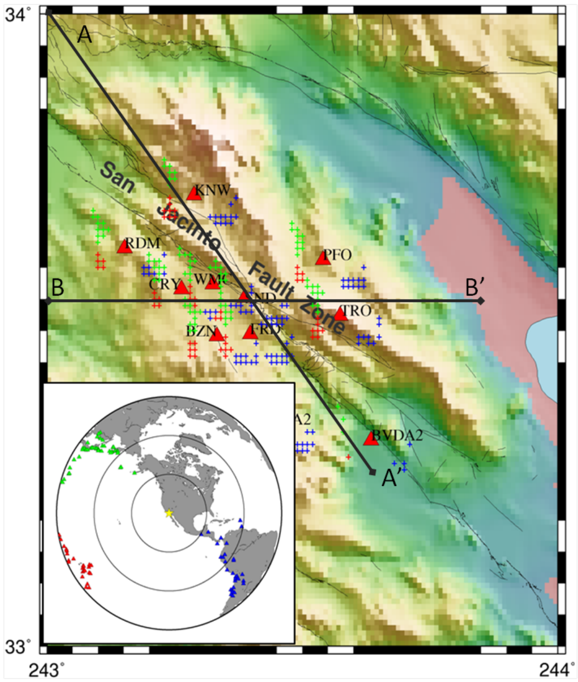

Figure 3. Topographic map of San Jacinto Fault Zone. Red triangles are AZ network stations used. Crosses are piercing points for the Ps converted waves at the 30-km-deep interface. The different colors represent different back azimuth bins, which are corresponding to figure 2. Red = 180-270deg; blue = 90- 180 deg; green = 270-360deg.

Initial results were presented at the 2010 AGU meeting asa poster presentation (Zhang et al, 2010) and the highlights are shown in Figures 3 and 4 for a few selected stations from the AZ (Anza) network. Stations PFO and CRY, which are at similar latitude but located on opposite sides of the fault, have conversion points (estimated at 30 km depth) that are clearly on either side of the surface trace. Receiver function plots clearly show the second positive arrival (Moho conversion) occurs at different Moho depths on either side of the fault (Figure 4). The Moho is at ~25 km beneath PFO (to the east of the SJF), whereas it is at ~30 km depth beneath CRY (to the west of the SJF). Depth variations for the Moho signal are also observed for different back azimuth bins for station KNW, near the San Jacinto fault and the southern segment of San Andreas fault (Figure 4).

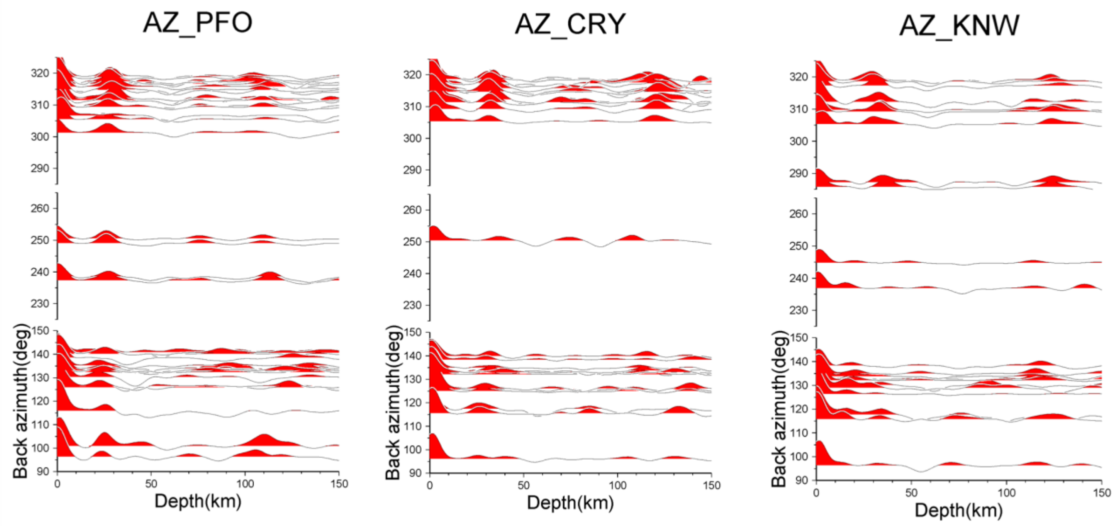

Figure 4. Receiver functions plotted by back azimuth at PFO, CRY, KNW stations near San Jacinto Fault. Receiver gathers at each side of the San Jacinto Fault (PFO and CRY) appear at different Moho depths. Receiver gathers at KNW appear strong azimuthal dependence on Moho depth due to the position of the conversion points relative to the surface trace of the fault.

Initial CCP stacking (Zhu, 2000; Chen et al., 2008) results for the San Jacinto fault also image the lithosphere and asthenosphere boundary (LAB) at approximately 60 km depth. These results indicate a sharply defined, ~8 km vertical step of the LAB beneath the San Jacinto fault near the Anza seismic gap (Figure 5). The vertical step in the LAB is constrained by the CCP stacking data to occur within a zone no wider than approximately10 km fault-perpendicular distance. The offset is probably related to juxtaposition by right-lateral strike-slip of LAB of different depths. The occurrence of this pronounced step directly beneath the surface trace of the San Jacinto fault suggests that the fault extends as a discrete shear zone through the entire lithosphere to a depth of at least 60 km, supporting the notion that the major strike-slip faults of the San Andreas system separate the lithosphere of southern California into discrete lithospheric blocks.

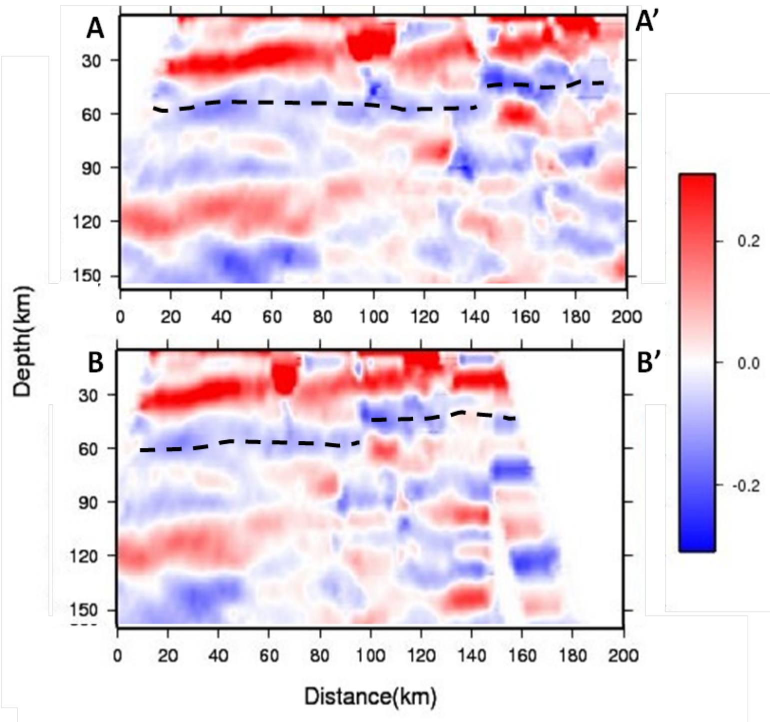

Figure 5. Common conversion points (CCP) stacks of P receiver functions along two cross sections AA', BB' as shown in Figure 3. The step of LAB is marked as black dash line.

Future work

As we continue to work on this project, we plan to systematically compare the lithospheric and crustal structure imaged with the receiver functions with: (1) earthquake locations; (2) geologic and geodetic slip rates; (3) long term geologic evolution of the region; (4) synthetic tests to determine resolution and potential artifacts; (5) and finally S receiver functions to image some of the obscured LAB features obscured by crustal multiples. Better definition the crustal and lithospheric structure in southern California has implications for fault loading, which may control spatio-temporal patterns of earthquake occurrence, as well as dynamical models of lithospheric deformation. A key advance in our proposed work will be the use of the SCEC community velocity model in a migration process to improve location accuracy, and the resulting Moho map will be a basic input to the next generation CVM.

References

Atwater, T. 1970. Implications of plate tectonics for the Cenozoic tectonic evolution of western North America. GSA Bulletin 81 (12): 3513.

Bailey, I.W., Miller, M.S., Liu, K., and Levander, A., 2010. Joint inversion of receiver function and phase velocity data for Vs structure beneath the Colorado Plateau, v. in preparation.

Chen, L., T. Zheng, and W. Xu, 2006, A Thinned Lithospheric Image of the Tanlu Fault Zone, Eastern China: Constructed from Wave Equation Based Receiver

Function Migration, J. Geophys. Res., 111, B09312, doi:10.1029/2005JB003974.

Chen, L., L. X. Wen, and T. Zheng, 2005, A Wave Equation Migration Method for Receiver Function Imaging, (II) Application to the Japan subduction zone, J. Geophys. Res., 110, B11310, doi:10.1029/2005JB003666.

Chen, L., L. X. Wen, and T. Zheng, 2005, A Wave Equation Migration Method for Receiver Function Imaging, (I) Theory, J. Geophys. Res., 110, B11309, doi:10.1029/2005JB003665.

Clayton, R.W. and Yan, Z. 2007. Regional mapping of the crustal structure in southern California from receiver functions. Journal of Geophysical Research - Solid Earth 112 (B5): B05311.

Grand, S.P., and Helmberger, D.V., 1984. Upper mantle shear structure of North America. Geophysical Journal International 76 (2): 399-438.

Langston, C.A., 1977, Corvallis, Oregon, crustal and upper mantle receiver structure from teleseismic P and S waves: Bulletin of the Seismological Society of America, v. 67, p. 713-724.

Miller, M.S. and Levander, A. 2009. Receiver function images of the Western U.S. lithosphere. Earthscope Onsite Newsletter. V. summer 2009, p. 2-3.

Miller, M.S. and Eaton, D.W. (2010), Formation of cratonic mantle keels by arc accretion: evidence from S-receiver functions, Geophysical Research Letters, 37, doi:10.1029/2010GL044366.

Miller, M.S., Levander, A., Niu, F., Li, A. (2009). Upper mantle structure beneath the Caribbean – South American plate boundary from surface wave tomography. J. Geophys. Res. 114, B01312, doi:10.1029/2007JB005507.

Vinnik, L.P., 1977, Detection of waves converted from P to SV in the mantle: Physics of the Earth and Planetary Interiors, v. 15, p. 1977.

Wdowinski, S., 2009. Deep creep as a cause for the excess seismicity along the San Jacinto fault. Nature Geoscience v. 2

Yan, Z, and Clayton, R.W. 2007. A notch structure on the Moho beneath the eastern San Gabriel mountains. Earth and Planetary Science Letters 260 (3-4): 570-81.

Zhang, P., Miller, M.S., and Dolan, J., 2010, Systematic mapping of the Moho beneath southern California, AGU Fall Meeting: San Francisco, CA, AGU.

Zhu, L., 2000, Crustal Structure across the San Andreas Fault, Southern California from Teleseismic Converted Waves, *Earth and Planetary Sci. Lett.*, 179, 183-190

Zhu, L.P. and Kanamori, H., 2000. Moho depth variation in southern california from teleseismic receiver functions. Journal of Geophysical Research- Solid Earth 105 (B2): 2969-80.

Zhu, L.P., 2002. Deformation in the lower crust and downward extent of the San Andreas Fault as revealed by teleseismic waveforms. Earth and Space, 54 (11): 1005-10.